



S0038-1098(96)00064-6

## VISIBLE PHOTOLUMINESCENCE FROM LOW TEMPERATURE DEPOSITED HYDROGENATED AMORPHOUS SILICON NITRIDE

Atilla Aydınli, Ali Serpengüzel and Diden Vardar

Department of Physics, Bilkent University, Bilkent, Ankara, 06533, Turkey

*(Received 25 September 1995; accepted 23 January 1996 by R. Fieschi)*

Hydrogenated amorphous silicon nitride ( $a\text{-SiN}_x\text{:H}$ ) samples have been prepared by plasma enhanced chemical vapor deposition (PECVD) using a mixture of silane ( $\text{SiH}_4$ ), nitrogen and ammonia ( $\text{NH}_3$ ). Most films exhibit visible photoluminescence (PL) and some emit strong PL after annealing. While films grown without  $\text{NH}_3$  exhibit PL in the deep red, those grown with  $\text{NH}_3$  show PL in the green. The PL properties of these films with no oxygen (O) content are similar to those of silicon oxide ( $\text{SiO}_x$ ) films and porous Si. Using infrared and X-ray Photoelectron Spectroscopy, we suggest that PL from  $a\text{-SiN}_x\text{:H}$  films originate from Si clusters which form during PECVD and crystallize upon annealing. We propose that the presence of O is not necessary for efficient PL.

Keywords: A. thin films, D. optical properties, E. luminescence.

Recently, strong room temperature luminescence of porous silicon (Si) obtained by both stain and anodically etched crystalline Si has been investigated. The process is promising for light emitting devices, since it can be tuned to different wavelengths<sup>1</sup>, and can be integrated into the existing Si microelectronics technology. The original proposal by Canham<sup>2</sup>, that light emission occurs due to carrier confinement in narrow columns of crystalline Si, has been challenged with the proposals of surface effects<sup>3</sup> and siloxene<sup>4</sup> as the source of light emission. In addition to the Si columns that form during the anodization process, both microcrystalline Si with average size of a few nanometers, and amorphous material have been observed<sup>5</sup>. The photoluminescence (PL) properties of porous Si have been attributed to Si columns, microcrystallites, and H and/or O containing amorphous material<sup>3</sup>. Amorphous hydrogenated Si ( $a\text{-Si:H}$ ) also shows visible PL at room temperature, when prepared by chemical vapor deposition<sup>6</sup>. Furthermore,  $a\text{-SiO}_x\text{:H}$  samples incorporating various concentrations of O have showed visible PL at room temperature<sup>7</sup>. Carrier recombination has been invoked to explain PL in such cluster structures embedded in amorphous material<sup>8</sup>. Since porous Si may contain all of these materials (i.e., Si columns, microcrystallites, and H and/or O containing amorphous material), it is to be suspected that the origin of PL in porous Si may be the same or similar to those observed in  $a\text{-Si:H}$  or  $a\text{-SiO}_x\text{:H}$ . Initial

experiments of low temperature oxidation of porous Si, showing poor PL intensities have been superseded by high temperature oxidation experiments, which gave strong visible luminescence at room temperature<sup>9</sup>. Furthermore, oxidation via boiling in water has resulted in blue PL from porous Si<sup>10</sup>. Therefore, it is of interest to study, whether a non-oxygen containing material like  $a\text{-SiN}_x\text{:H}$  has the same PL properties as porous Si and Si rich  $a\text{-SiO}_x\text{:H}$ .

In this Communication, we present the results of PL and Fourier Transform Infrared (FTIR) characterization of both as-grown and rapid thermal processor (RTP) annealed  $a\text{-SiN}_x\text{:H}$  deposited by plasma enhanced chemical vapor deposition (PECVD). X-ray Photoelectron Spectroscopy was also employed to determine the valency of Si and N.

$a\text{-SiN}_x\text{:H}$  samples have been prepared on (001) Si substrates by PECVD at 100 °C with nitrogen ( $\text{N}_2$ ) balanced 2% silane ( $\text{SiH}_4$ ), and pure ammonia ( $\text{NH}_3$ ) as the source. Other substrates such as quartz were not used to avoid the possibility of O uptake from the substrate during high temperature annealing. No intentional O was introduced into the chamber. The flow ratio of  $\text{NH}_3/[(2\%\text{SiH}_4+98\%\text{N}_2)+\text{NH}_3]$  defined as  $R$ , was varied from 0 to 0.2. The rf power and chamber pressure were 10 W and 1 Torr, respectively. The thicknesses of the samples were

kept at approximately 500 nm. Annealing was done immediately in forming gas environment using a RTP for 10 minutes up to 800 °C with 100 °C intervals. PL was measured at room temperature using a 1-m double monochromator, equipped with a cooled GaAs PMT and standard photon counting electronics. For PL excitation the 457.9 nm and 514.5 nm lines of an Ar<sup>+</sup> laser were used.

Figure 1 shows the IR spectra of samples deposited with differing values of *R* ranging from *R*=0 to *R*=0.2. Several peaks are readily identified as SiN-H<sub>2</sub> stretching (~3450 cm<sup>-1</sup>), Si<sub>2</sub>N-H stretching (~3350 cm<sup>-1</sup>), N<sub>2</sub>Si-H stretching (~2150 cm<sup>-1</sup>), SiN-H<sub>2</sub> bending (~1550 cm<sup>-1</sup>), and Si<sub>2</sub>N-H rocking (~1170 cm<sup>-1</sup>) modes. The reactive nature of NH<sub>3</sub> becomes obvious, when IR spectra of samples grown with and without NH<sub>3</sub> are compared. For the samples grown with *R*=0, we observe very weak Si<sub>2</sub>N-H stretching and rocking modes. As *R* increases, the Si<sub>2</sub>N-H modes become stronger. In fact, careful inspection of the spectra shows that increasing *R* results in an increase of (Si bonded) N-H bonds, and a decrease of Si-H bonds. It is possible to estimate Si-H and (Si bonded) N-H bond concentrations using the absorbances at ~2150 cm<sup>-1</sup> and ~3350 cm<sup>-1</sup>, respectively<sup>11</sup>. We find that for as-grown samples with *R*=0, Si-H concentration is 3.3×10<sup>22</sup> cm<sup>-3</sup>, while N-H concentration is 2.3×10<sup>21</sup>cm<sup>-3</sup>. Addition of NH<sub>3</sub> changes this drastically, reducing the Si-H concentration by a factor of 3, while increasing the N-H concentration by more than an order of magnitude to 3.5×10<sup>22</sup> cm<sup>-3</sup>, for samples grown with *R*=0.05.

In Fig.1, the region of 800-900 cm<sup>-1</sup> may have contributions from several sources. Since the

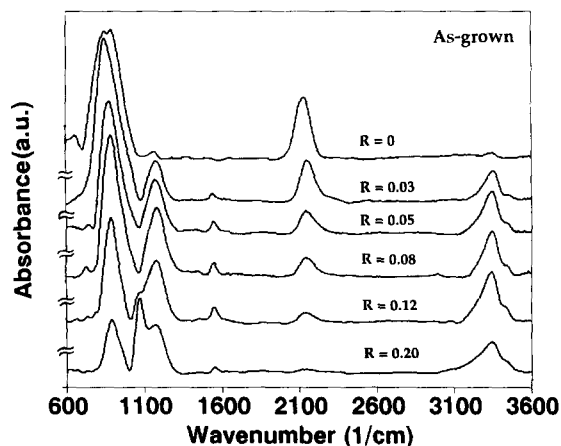


Fig. 1. IR absorption spectra of as grown a-SiN<sub>x</sub>:H films as a function of *R*. The spectra were taken within 24 hours of growth.

deposition temperature was 100 °C, as-grown samples may contain polysilanes<sup>12</sup>. A detailed analysis to differentiate among various bonding configurations of Si-H shows that, peaks at 2000 cm<sup>-1</sup> and 630 cm<sup>-1</sup> are due to monohydrides (SiH), 2090 cm<sup>-1</sup>, 875 cm<sup>-1</sup>, 630 cm<sup>-1</sup> to disilanes (SiH<sub>2</sub>), 2100 cm<sup>-1</sup>, 890 cm<sup>-1</sup>, 845 cm<sup>-1</sup>, 630 cm<sup>-1</sup> to (SiH<sub>2</sub>)<sub>n</sub>, and 2140 cm<sup>-1</sup>, 907 cm<sup>-1</sup>, 862 cm<sup>-1</sup>, 630 cm<sup>-1</sup> to SiH<sub>3</sub>.<sup>13</sup> This analysis suggests the presence (SiH<sub>2</sub>)<sub>n</sub> in our samples. However, contributions of the Si-N in plane stretching vibration starting at 840 cm<sup>-1</sup> and shifting up to 890 cm<sup>-1</sup> is also in the same range. In the case of the *R*=0 sample, we observe that, the contribution of the polysilanes around the Si-N in plane stretching vibration decreases as we anneal the samples up to 800 °C (not shown). In fact, as soon as *R* becomes ≥0.02, the contribution of the polysilanes to the peak at 855 cm<sup>-1</sup> is no longer distinguishable. This peak shifts to higher frequencies, as NH<sub>3</sub> concentration is increased. At higher concentrations of NH<sub>3</sub>, we also witness the appearance of a peak at 1074 cm<sup>-1</sup> (*R*=0.12 and 0.2), which we do not observe at lower concentrations of NH<sub>3</sub> (*R*<0.12). This peak is identified as the antisymmetric stretching mode of Si-O-Si. This is not unusual, since these FTIR measurements were done within 24 hours of growing the samples, and it is known that at high concentrations of NH<sub>3</sub> rapid oxidation of low temperature deposited a-SiN<sub>x</sub>:H takes place.<sup>13</sup> However, we note that, a-SiN<sub>x</sub>:H films become resistant to oxidation (for at least up to four months) after annealing at temperatures above 600 °C.

Figure 2 shows the IR spectra of samples with *R*=0.05 annealed from 400 °C to 800 °C. Each annealing was done on a separate sample. In these

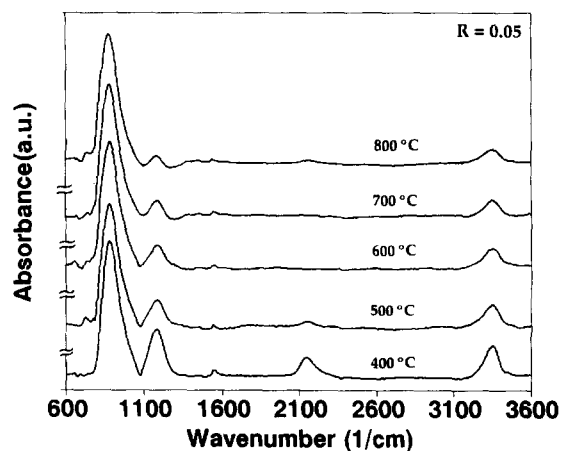


Fig. 2. IR absorption spectra of samples grown with *R*=0.05 and annealed at various temperatures.

samples in addition to the dominant Si-N in plane stretching mode ( $\sim 880\text{ cm}^{-1}$ ), we also observe the Si<sub>2</sub>N-H rocking ( $\sim 1170\text{ cm}^{-1}$ ), the SiN-H<sub>2</sub> bending ( $\sim 1550\text{ cm}^{-1}$ ), the N<sub>2</sub>Si-H stretching ( $\sim 2150\text{ cm}^{-1}$ ), and the Si<sub>2</sub>N-H stretching mode ( $\sim 3350\text{ cm}^{-1}$ ). As the annealing temperature is increased, we observe the effusion of H through the decrease of N-H and Si-H related peaks ( $\sim 3350\text{ cm}^{-1}$ ,  $\sim 2150\text{ cm}^{-1}$ ,  $\sim 1550\text{ cm}^{-1}$ , and  $\sim 1170\text{ cm}^{-1}$ ). However, while most of the Si bonded H is driven out during annealing (as evidenced by a very weak peak at  $\sim 2150\text{ cm}^{-1}$ ), a lot of N-H bonds are still intact<sup>14,15</sup> even after  $800^\circ\text{C}$  annealing (note the remaining Si<sub>2</sub>N-H peaks at  $\sim 3350\text{ cm}^{-1}$  and  $\sim 1170\text{ cm}^{-1}$ ). We have also estimated Si-H and N-H bond concentrations as a function of annealing temperature. We find that annealing the samples grown with  $R=0.05$  at  $800^\circ\text{C}$  reduces Si-H concentration by a factor of 10, and the N-H concentration by only a factor of 3. This is to be expected, since the N-H bond energy is  $4.05\text{ eV}$ , while the Si-H bond energy is  $3.1\text{ eV}$ .<sup>16</sup>

Figure 3 shows the room temperature PL spectra of the samples of Fig. 2 (with  $R=0.05$  annealed from  $400^\circ\text{C}$  to  $800^\circ\text{C}$ ). PL peak position from as-grown samples with  $R>0$  is in the vicinity of  $500\text{ nm}$ . The FWHM of these spectra are typically about  $0.5\text{ eV}$ . In the inset of Fig. 3, we show the observed red shift of the PL peak position upon annealing for samples with  $R=0.05$ . The data for the PL peak position is compiled from four sets of samples grown and annealed under the same conditions. Even though there is some scatter in the data (as shown with a bar

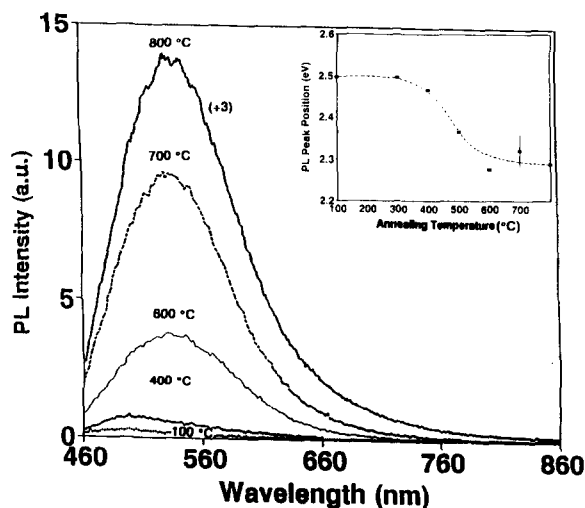


Fig.3. PL spectra of samples grown with  $R=0.05$  annealed at various temperatures. The PL peak position as a function of annealing temperature is given in the inset. The typical standard deviation of the data is shown for the data point at  $700^\circ\text{C}$ .

for the data point at  $700^\circ\text{C}$ ), the red shift upon annealing is evident. After annealing at and above  $600^\circ\text{C}$ , the samples with  $R=0.05$  exhibit PL strong enough to be observed by the naked eye. For one set of samples, special attention was paid to perform both the FTIR and the PL spectroscopy immediately after the growth and annealing to clearly establish the presence of the PL before any oxygen contamination could take place. While we can not entirely rule out the presence of O on the microscopic level, the fact that, high temperature annealed samples do not show signs of O contamination as detected by FTIR, lead us to conclude that O does not play a significant role in the mechanism resulting in visible PL. However, we note that partially oxidized samples at lower temperatures also exhibit visible PL.

We have also recorded the PL spectra of samples with  $R=0$  (Fig.4). The spectra have been normalized to emphasize the shifts in the PL peak position. These samples, have broader PL spectra extending from the blue to near-IR, which are similar to porous Si<sup>3</sup>. The PL spectrum for the as grown sample peaks around  $695\text{ nm}$ . The peak red shifts up to  $750\text{ nm}$  upon annealing up to  $400^\circ\text{C}$ , while preserving the general shape of the PL spectra. The PL spectrum of the sample annealed at  $400^\circ\text{C}$  has a tail extending to  $900\text{ nm}$  (the limit of our detection system). These samples do not exhibit any PL signal, within our spectral detection range, when annealed at  $500^\circ\text{C}$  or higher temperatures. The loss of PL signal upon annealing at  $500^\circ\text{C}$  and higher temperatures correlates well with the effusion of H from these samples as deduced from FTIR measurements (not shown). In the FTIR measurements of the samples annealed at  $500^\circ\text{C}$ , we find that, Si-H concentration

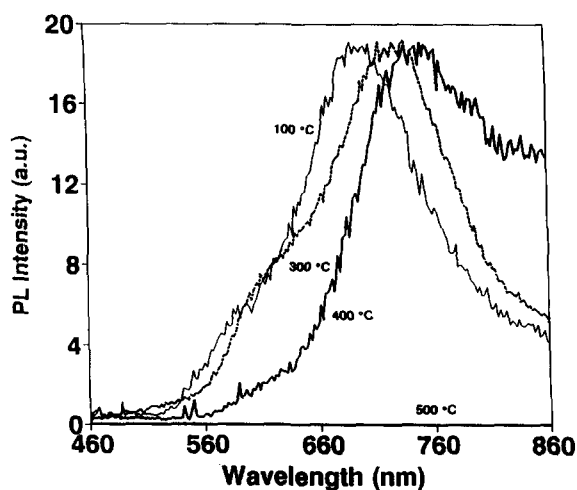


Fig.4. PL spectra of samples grown with  $R=0$  and annealed up to  $500^\circ\text{C}$ .

decreases by a factor of 5.8 while the already weak N-H concentration falls below our detection limit.

In order to understand the valency of the Si and N making up the samples, XPS analysis (not shown) of samples grown with  $R=0$  and 0.05 was also performed. The Si 2p spectra of both as-grown and 800 °C annealed samples were compared. In the case of the as-grown sample with  $R=0.05$ , we observe a well resolved single symmetric peak centered at 104 eV; for the same sample annealed at 800 °C, we observe two peaks: one centered at 104 eV, and another small one at 100 eV. The large peak at 104 eV represents the bonded Si. The small peak at 100 eV, whose binding energy compares well with the corresponding Si 2p peak for bulk Si (99.12 eV), establishes the presence of zero valent Si. Note that binding energy of zero valent Si in SiN<sub>x</sub> is upshifted from that of Si 2p in bulk Si<sup>19</sup>. The low energy Si 2p peak is also present much more strongly in both the as-grown and the annealed samples grown with  $R=0$ , again pointing to the presence of zero valent Si.

In Fig. 5, we display the PL peak intensity as a function of  $R$ . In general, we observe that for all compositions with  $R \neq 0$ , increasing annealing temperatures lead to increasing PL intensities. We also observe that, in the vicinity of  $R=0.05$ , there is a sharp increase of the PL peak intensity for all annealing temperatures. The only exception to this are the samples grown with  $R=0$ . For as-grown samples we observe PL in the deep red which shows a five fold increase upon annealing at 300 °C, falling sharply when annealed at 400 °C. At 500 °C and higher temperatures, PL intensity is either totally quenched or shifts beyond 900 nm (spectral limit of our monochromator) with much reduced

intensity. We also note that increasing  $R$  values beyond  $R=0.05$  decreases PL intensity, which correlates well with decreasing Si-H bond concentration.

We begin interpreting our data for samples grown with  $R=0$ . It is known that, a-SiN<sub>x</sub>:H films deposited on low temperature substrates show columnar growth morphology with material in the columns assumed to be a-Si with isolated N atom bonding sites<sup>17</sup>. The connecting material between the columns is (SiH<sub>2</sub>)<sub>n</sub>. Such a picture, is not inconsistent with the model proposed by Brodsky<sup>8</sup> as well as the observation of Bruesch et.al.<sup>18</sup> in the case of a-SiO<sub>x</sub>:H. We propose that, our samples consist of small a-Si clusters in a matrix of a-Si:H and a-SiN<sub>x</sub>:H. The regions with Si-N and Si-H, having larger energy gaps due to strong Si-H and Si-N bonds, isolate these a-Si clusters, and form barrier regions around them. The weak PL, which is observed in the deep red originates from these a-Si clusters. With increasing annealing temperatures, PL becomes stronger due to crystallization of the clusters and shifts into the IR due to H effusion and increasing crystallite size. Further increase of the annealing temperature results in the increase of the crystallite size, causing the quenching of the visible and near-IR PL. At this point, we believe that, most of the Si crystallites are large enough to show bulk-like behavior and no longer luminesce in the visible. This picture is further supported by the presence of zero valent Si in the XPS data of the samples with  $R=0$  both before and after annealing. In fact the very broad XPS peak, which is observed from the as-grown samples, is actually composed of multiple peaks corresponding to bonded and zero valent Si.

Addition of NH<sub>3</sub> into the chamber changes the situation dramatically. First, we observe from the FTIR data that, both H and N uptake of the samples during the growth increases. Second, the PL peak position shifts to shorter wavelengths (~500 nm) by more than 150 nm. We find that, annealing the samples increases PL efficiency, which again correlates well with H effusion. However, we find that, there still remains much H in the samples, as evidenced by the presence of large amounts of Si<sub>2</sub>N-H bonds at ~3350 cm<sup>-1</sup>, which we believe limits the size of the clusters during growth. Considering this together with the XPS data for  $R=0.05$  samples, we propose that the a-Si clusters are now smaller due to the presence of large amounts of Si-H and N-H, which limits the growth of the clusters, which are now separated by a stronger matrix of a-Si:H and a-SiN<sub>x</sub>:H. This explains the shorter wavelength PL peak position of  $R=0.05$  samples when compared with the samples with  $R=0$ . The fact that, a lot of H through Si<sub>2</sub>N-H still remains in the samples, explains the small red shifts observed upon

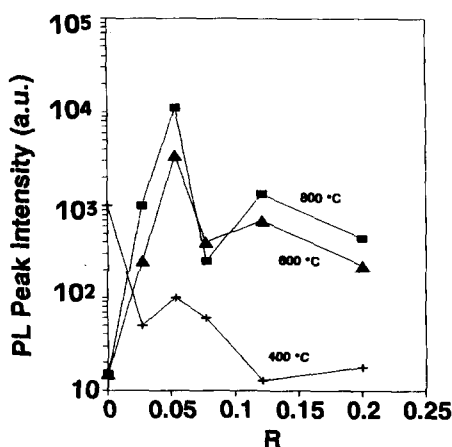


Fig.5. PL peak intensity as a function of the flow ratio  $R$  for various annealing temperatures.

annealing.

In conclusion, samples grown without NH<sub>3</sub> show PL in the near-IR, while those grown with NH<sub>3</sub> have PL in the green. Samples with R>0 exhibit PL, which becomes stronger with annealing. In particular, samples grown with R=0.05 give strong visible PL, when annealed. Since no intentional O was introduced during the growth and annealing, we conclude that O is not a necessary component of the PL mechanism. We suggest that, PL originates from Si clusters of differing sizes in common with similar

results in a-SiO<sub>x</sub>:H.<sup>7</sup> These clusters are smaller in the case of samples grown with R>0. High temperature annealing leads to increases in the sizes of these clusters as well as improving the crystallinity.

We are grateful to Prof. Şefik Süzer of the Chemistry Department for XPS measurements, Murat Güre for help with the sample preparation. We also gratefully acknowledge the support of this research by the Scientific and Technical Research Council of Turkey (TUBITAK) through Grant No : TBAG-1244.

### References

1. A. Bsiesy et al. Surf. Sci. **254**, 195 (1991).
2. L.T. Canham, Appl. Phys. Lett. **57**, 1046 (1990).
3. Optical Properties of Low Dimensional Silicon Structures, NATO ASI Series, **44**, Eds:D.C.Bensahel, L.T.Canham, and S.Ossicini, Dordrecht, Kluwer (1993).
4. M.S.Brandt, H.D.Fuchs, M.Stutzmann, J.Weber, and M. Cardona, Solid State Commun. **81**, 307 (1992).
5. M.W.Cole, J.F.Harvey, R.A.Lux, D.W.Eckert and R.Tsu, Appl. Phys. Lett. **60**, 2800 (1992).
6. D.J.Wolford, B.A. Scoot, J.A. Reimer and J.A.Bradley, Physica **B117**, 920 (1983).
7. F.N.Timofeev, A.Aydinli, R. Ellialtıoğlu, K. Türkoğlu, M. Güre, V.N.Mikhailov, and O.A. Lavrova, Solid State Commun. **95**, 443 (1995).
8. M.H.Brodsky, Solid State Commun. **36**, 55 (1980).
9. V. Petrova-Koch, T. Muschik, A. Kux, B.K.Meyer and F. Koch, Appl. Phys. Lett. **61**, 943 (1992).
10. X.Y.Hou, G.Shi, W. Wang, HF.L.Zhang, P.H.Hao, D. M.Huang and X.Wang, Appl. Phys. Lett. **62**, 1097 (1993).
11. W.A.Lanford, and M.J.Rand, J.Appl. Phys. **49**, 2473 (1978).
12. W. B. Pollard, and G.Lucovsky, Phys. Rev. **B26**, 3172 (1982).
13. W.-S. Liao, C.-H. Lin and S.-C. Lee, Appl. Phys. Lett. **65**, 2229 (1994).
14. A. Morimoto, S. Oozara, M. Kumeda and T. Shimizu, Phys. Status Solidi **B119**, 715 (1983)
15. H.J.Stein, P.S.Peercy and R.J.Sokel, Thin Solid Films **101**, 291 (1983).
16. J. Robertson, Philosophical Magazine **B69**, 307 (1994).
17. G. Lucovsky, J. Yang, S.S.Chao, J.E.Tyler, and W. Czubatyj, Phy. Rev. **B28**, 3243 (1983).
18. P.Bruesch, Th.Stockmeier, F.Stucki, P.A.Buffat, and J.K.N. Linder, J. Appl. Phys. **73**, 7677 (1993).
19. R.Karcher, L.Ley and R.L.Johnson, Phys. Rev.B, **30**, 1896 (1984).